The Tmc Complex from Desulfovibrio vulgaris Hildenborough Is Involved in Transmembrane Electron Transfer from Periplasmic Hydrogen Oxidation †

ARTICLE *in* BIOCHEMISTRY · SEPTEMBER 2006

Impact Factor: 3.02 · DOI: 10.1021/bi0610294 · Source: PubMed

The Tmc Complex from *Desulfovibrio vulgaris* Hildenborough Is Involved in Transmembrane Electron Transfer from Periplasmic Hydrogen Oxidation†

Patrícia M. Pereira, Miguel Teixeira, António V. Xavier, Ricardo O. Louro, and Inês A. C. Pereira*

Instituto de Tecnologia Química e Biológica, Universidade Nova de Lisboa, 2781-901 Oeiras, Portugal

Received May 24, 2006; Revised Manuscript Received July 10, 2006

ABSTRACT: Three membrane-bound redox complexes have been reported in *Desulfovibrio* spp., whose genes are not found in the genomes of other sulfate reducers such as *Desulfotalea psycrophila* and *Archaeoglobus fulgidus.* These complexes contain a periplasmic cytochrome *c* subunit of the cytochrome c_3 family, and their presence in these organisms probably correlates with the presence of a pool of periplasmic cytochromes c_3, also absent in the two other sulfate reducers. In this work we report the isolation and characterization of the first of such complexes, Tmc from *D. vulgaris* Hildenborough, which is associated with the tetraheme type II cytochrome c_3. The isolated Tmc complex contains four subunits, including the TpIIc_3 (TmcA), an integral membrane cytochrome *b* (TmcC), and two cytoplasmically predicted proteins, an iron−sulfur protein (TmcB) and a tryptophan-rich protein (TmcD). Spectroscopic studies indicate the presence of eight hemes *c* and two hemes *b* in the complex pointing to an $\alpha_2\beta\gamma\delta$ composition ($TmcA_2BCD$). EPR analysis reveals the presence of a $[4Fe4S]^{3+}$ center and up to three other iron−sulfur centers in the cytoplasmic subunit. Nearly full reduction of the redox centers in the Tmc complex could be obtained upon incubation with hydrogenase/TpIc_3, supporting the role of this complex in transmembrane transfer of electrons resulting from periplasmic oxidation of hydrogen.

Sulfate-reducing organisms (*1*) are anaerobic prokaryotes found ubiquitously in nature. They employ a respiratory mechanism with sulfate as the terminal electron acceptor giving rise to sulfide as the major metabolic end product. As energy source, they can generally use organic acids, alcohols, or molecular hydrogen for sulfate reduction. These organisms play an important role in global cycling of sulfur and other elements, as for example carbon, since they form part of microbial consortia that completely mineralize organic carbon in anaerobic environments (*2*).

Sulfate reduction is a true respiratory process, which leads to oxidative phosphorylation through a still incompletely understood electron transfer pathway. This electron transport chain links dehydrogenases to the terminal reductases located in the cytoplasm and displays significant differences from other modes of anaerobic respiration like the reduction of nitrate or methanogenesis. Energy conservation mechanisms require that cytoplasmic sulfate reduction is coupled to membrane-associated electron transport, and several membrane-bound electron transfer complexes have been identified that are likely to be involved in this function (*3*). Analysis of available genomes for sulfate-reducing organisms [three bacteria, *Desulfovibrio vulgaris* Hildenborough (*4*), *Desulfovibrio desulfuricans* G20[1] (www.jgi.doe.gov), and *Desulfotalea psychrophila* (*5*), and one archaeon, *Archaeoglobus fulgidus* (*6*)] reveals that only two membrane-bound electron transfer complexes are strictly conserved among them, suggesting that only these are essential for sulfate respiration. They are the three-subunit Qmo complex (*7*) and the five-subunit Dsr complex encoded by the *dsr*MKJOP genes in *Desulfovibrio* (*8*, *9*) and named Hme in *A. fulgidus* (*10*). The Qmo[2] complex is likely to be involved in electron transfer from the quinone pool to APS reductase (*7*, *8*, *11*), whereas the Dsr complex is likely to channel electrons from the periplasm and quinone pool to the sulfite reductase (*7*−*9*, *11*).

Most research on the metabolism and biochemistry of sulfate reducers has been done with members of the genus *Desulfovibrio* (of the δ-subgroup of proteobacteria). *Desulfovibrio* spp. have some characteristics that are not shared with other sulfate-reducing organisms, including a pool of numerous periplasmic cytochromes *c* (*4*), of which the most abundant is the well-known type I cytochrome c_3 (TpIc_3) (reviewed in ref *12*). These cytochromes *c* act as electron acceptors for periplasmic hydrogenases and formate dehydrogenases. In *Desulfovibrio* these two classes of proteins lack the heme *b*-containing membrane subunit typically present in such enzymes and which transfers electrons to the quinone pool. The electrons resulting from periplasmic oxidation of hydrogen or formate are likely to be transferred from the cytochrome c_3 pool to one of several membrane-

† This work was supported by Fundação para a Ciência e Tecnologia Grants POCTI/2002/ESP/44782 to I.A.C.P., POCTI/2002/QUI/47866 to A.V.X., POCTI/2002/BME/37406 to M.T., and POCI/2004/QUI/55690 to R.O.L., cofunded by the FEDER program. P.M.P. was a recipient of FCT PhD Grant SFRH/BD/5231/2001.

* To whom correspondence should be addressed. Tel: 351-214469327. Fax: 351-214411277. E-mail: ipereira@itqb.unl.pt.

[1] *D. desulfuricans* G20 has to be reclassified as it is not actually a *desulfuricans* spp. (*7*, *9*).

[2] Abbreviations: Qmo, quinone-interacting membrane-bound oxidoreductase complex; *Dv*H, *Desulfovibrio vulgaris* Hildenborough; TpIIc_3, type II cytochrome c_3; Hmc, high molecular mass cytochrome; 9Hc, nine-heme cytochrome *c*; DDM, *n*-dodecyl β-D-maltoside; DMN, 2,3-dimethyl-1,4-naphthoquinone.

10.1021/bi0610294 CCC: $33.50
Published on Web 08/05/2006

bound electron transfer complexes found only in *Desulfovibrio*, which include a cytochrome *c* subunit also belonging to the cytochrome c_3 family (reviewed in ref *3*). These membrane redox complexes are not present in *Dt. psychrophila* and *A. fulgidus*, which have hydrogenases and formate dehydrogenases with a cytochrome *b* membrane subunit. The first of such *Desulfovibrio* complexes to be identified was the six-subunit Hmc complex of *D. vulgaris* (*13*). Sequence analysis indicates that this complex includes a cytoplasmic FeS protein (HmcF), two integral membrane proteins of which one is likely to bind hemes *b* (HmcC and HmcE), a periplasmic ferredoxin-like protein (HmcD), and a periplasmic 16-heme cytochrome *c* (HmcA) composed of four cytochrome c_3-like domains (*14, 15*). Expression of the Hmc complex is higher in growth with H_2 (*16*), and studies with knock-out mutants (*17, 18*) and on reduction of HmcA by hydrogenase/TpIc_3 (*19*) indicate that the Hmc complex is involved in electron transfer from periplasmic hydrogen oxidation to cytoplasmic sulfate reduction.

Two homologous, but smaller complexes have since been identified in *Desulfovibrio* spp. The 9Hc complex of *D. desulfuricans* ATCC 27774 (*20*) lacks the heme *b* and cytoplasmic FeS subunits of Hmc but is formed by an integral membrane subunit (9HcC) and a periplasmic FeS subunit (9HcB) that display high sequence identity to the corresponding subunits of Hmc. It is also associated with a nine-heme cytochrome (9HcA), whose sequence and structure are very similar to the C-terminal domain of the HmcA cytochrome (*21*). In *D. vulgaris* and *D. desulfuricans* G20, another transmembrane complex, Tmc, was identified that includes a cytochrome *b* integral membrane subunit homologous to HmcE, a cytoplasmic FeS subunit homologous to HmcF and of the same family as DsrK, and a periplasmic tetraheme cytochrome *c*, named as type II cytochrome c_3 (TpIIc_3), which differs from the TpIc_3 in reactivity and structural characteristics (*22, 23*). The cytochrome *c* subunits of the Hmc, 9Hc, and TpIIc_3 complexes have already been purified and characterized, but a whole complex of this family had hitherto not been isolated. The three cytochromes, HmcA, 9HcA, and TpIIc_3, can receive electrons from periplasmic hydrogenases via the TpIc_3 (reviewed in ref *3*), supporting the idea that the corresponding complexes transfer electrons from the periplasmic oxidation of hydrogen (and possibly also formate) to the membrane quinone pool or the cytoplasm. In this paper, we describe the purification and detailed characterization of the *D. vulgaris* Tmc complex associated with TpIIc_3 and studies that corroborate its proposed involvement in transmembrane electron transfer in hydrogen metabolism.

MATERIALS AND METHODS

Sequence Analysis Tools. Blast searches were performed at the NCBI website (http://www.ncbi.nlm.nih.gov/BLAST/). Sequence data were retrieved and analyzed at The Institute for Genomic Research website (http://www.tigr.org), at the DOE Joint Genome Institute website (http://www.jgi.doe.gov/JGI_microbial/html/index.html), and at the VIMSS Comparative Genomics website (http://www.microbesonline.org/). Multiple alignments were performed using CLUSTALX. Sequence analysis and transmembrane helix predictions were done using programs available at http://us.expasy.org/.

Bacterial Growth. Cells of *D. vulgaris* Hildenborough (DSM 644) were grown in lactate/sulfate medium as previously described (*24*). The cells were suspended in 10 mM Tris-HCl (pH 7.6) buffer and ruptured by passing twice through a APV 750 homogenizer. The resulting extract was centrifuged at a force of 10000*g* for 15 min to remove cell debris, and the supernatant was centrifuged at a force of 100000*g* for 2 h to obtain the crude membrane fraction.

Protein Purification. All purification steps were conducted aerobically and performed at pH 7.6 and 4 °C. The crude membrane fraction from *D. vulgaris* was washed by suspending in 20 mM Tris-HCl with 20% glycerol and 1 mM EDTA and ultracentrifuging at 140000*g* for 2 h. The pellet obtained was solubilized in a 20 mM Tris-HCl buffer containing 20% glycerol and 4% *n*-dodecyl β-D-maltoside (DDM), in the presence of Complete protease inhibitor cocktail tablets (Roche Diagnostics GmbH, Germany). Solubilization was carried out for 1.5 h in an ice bath with gentle stirring. The solubilized protein was separated by ultracentrifugation at 140000*g* for 2 h, and the pellet was used for a second solubilization using the same conditions as described before. The total solubilized protein was applied to a Q-Sepharose fast-flow column (5 × 30 cm; Pharmacia) equilibrated with 20 mM Tris-HCl buffer with 20% glycerol, 0.1% DDM (buffer A), and a quarter of a Complete tablet per liter. A stepwise gradient of increasing NaCl concentration was performed. Fractions were analyzed by UV−visible spectroscopy to search for the presence of both hemes *b* and *c* in the same sample. A fraction with such characteristics eluted at around 350 mM NaCl. This fraction was concentrated and dialyzed against buffer A and then loaded on a Pharmacia Q-Sepharose high-performance column (Hiload 26/10, flow rate 2 mL min^{-1}) equilibrated with buffer A and a quarter of a Complete tablet per liter. A stepwise gradient of increasing NaCl concentration was performed, and two heme-containing fractions were selected: one eluted at 100 mM NaCl and the other eluted at 1 M NaCl. These fractions were pooled and concentrated in an Amicon ultrafiltration cell using membranes with molecular cutoffs of 30 kDa.

Analytical Methods. Protein concentration was determined with the bicinchoninic acid assay from Pierce, using bovine serum albumin as standard. Blue-native PAGE was performed as described in ref *25* with the modification that the α-aminocaproic acid was not used in the gel buffer since this did not affect the electrophoresis pattern observed. Coomassie blue-stained SDS−PAGE was performed to determine the protein purity. For band quantification the SDS−PAGE stained with Coomassie blue was scanned and analyzed by densitometry using Quantity One software (Bio-Rad). To normalize the signal intensities, the low molecular mass markers (GE Healthcare) were used for a calibration curve. For N-terminal sequencing the subunits were separated by SDS−PAGE and blotted to a PVDF membrane (Millipore) using a Trans-Blot SD semidry electrophoretic transfer cell (Bio-Rad). Sequencing was conducted in an Applied Biosystems model Procise 491 HT sequencer. The pyridine hemochrome derivative was prepared as described in ref *26*.

Spectroscopic Methods. Room temperature UV−visible spectra were obtained using a Shimadzu UV-1603 spectrophotometer. Liquid nitrogen temperature spectra were obtained in an OLIS DW-2 instrument. EPR spectra were recorded using a Bruker EMX spectrometer equipped with

an ESR 900 continuous-flow helium cryostat from Oxford Instruments, as described (*27*). For reduction experiments, the Tmc complex was flushed with hydrogen and reduced with preactivated [NiFeSe] hydrogenase from *D. vulgaris* or, alternatively, with sodium dithionite.

Quinone−Tmc Interaction Experiments. The interaction was measured as the rate of quinone reduction by the reduced Tmc complex using an OLIS DW-2 spectrophotometer. All of the experiments were performed in anaerobic stirred cells, with a hydrogen overpressure of 15 kPa flowing through the cell. The buffer used in all cases was 100 mM Tris-HCl (pH 7.6). An ethanolic solution of 2,3-dimethyl-1,4-naphthoquinone (DMN) (140 μM) was incubated in the cell in degassed buffer with 115 units/μL catalase, 4 units of glucose oxidase, and 450 mg/mL glucose during 10 min. The Tmc complex was reduced using active [Fe], [NiFe], or [NiFeSe] hydrogenases from *D. vulgaris* and added to the cell at a 20 nM concentration. Reduction of DMN was followed using the optical density difference between 290 and 270 nm as described in the literature (*28*).

For the reverse reaction, DMN was reduced to $DMNH_2$ in a Braun MB 150 glovebox with sodium borohydride, according to ref *29*. The borohydride was added stepwise until full reduction occurred, following the process spectrophotometrically. $DMNH_2$ was added to the protein solution (2.8 μM) inside the anaerobic chamber to the final concentration of 237 μM. Spectra were recorded in a Shimadzu UV-1203 spectrophotometer. Afterward, an excess of sodium dithionite was added. As a control experiment an identical protein solution was treated with the same excess of sodium borohydride, in the absence of $DMNH_2$.

Redox Titration. Redox titrations monitored by visible spectroscopy were performed in the glovebox in 100 mM Tris−maleate, pH 7.0, buffer, following the changes in absorbance at the α and Soret bands of the reduced hemes, corrected for the corresponding isosbestic points, and using buffered sodium dithionite (pH 8.5) as the reductant. The following redox mediators were used (at a final concentration of 2.7 μM each): phenazine methosulfate, phenazine ethosulfate, methylene blue, indigo tetrasulfonate, indigo trisulfonate, indigo disulfonate, 2-hydroxy-1,4-naphthoquinone, anthraquinone-2-sulfonate, safranine-O, benzyl viologen, and methyl viologen. The reduction potentials were measured with a combined Pt/Ag/AgCl electrode calibrated against a saturated quinhydrone solution at pH 7 and are referenced to the standard hydrogen electrode. To discriminate the contribution of hemes *b* and *c* to the overall titration of the Tmc, the analysis of the redox titration was performed at 552 and 561 nm using the absorbance of isosbestic points at 540 and 561 nm and 504 and 570 nm, respectively, to deconvolute the optical contribution of the redox mediators from that of the two types of hemes.

Cross-Linking Reactions. Cross-linking reactions were performed aerobically with the oxidized Tmc complex or inside a glovebox with the Tmc complex in the reduced state. This state was obtained by adding a stoichiometric amount of dithionite to the Tmc complex (40 μM). Tmc was incubated for 1.5 h at room temperature in the reaction mixture containing 10 mM cacodylate buffer (pH 6), 10 mM EDC [1-[3-(dimethylamino)propyl]-3-ethylcarbodiimide hydrochloride], and either APS reductase (40 μM) or sulfite reductase (40 μM) from *D. vulgaris*. The reactions were stopped by adding ammonium acetate (pH 5) to 100 mM final concentration. The cross-linking reactions were analyzed by electrophoresis on polyacrylamide gel under denaturing conditions on a 12% gel (Hoefer SE 260). For identification, the gel was stained with Coomassie blue.

Biosensor Analysis. The interaction between the Tmc complex with TpIc_3, APS reductase, and sulfite reductase was investigated by surface plasmon resonance with the biosensor-based BIAcore analytical system. All experiments were performed at 25 °C. The Tmc complex in 10 mM sodium acetate (pH 4.5) was immobilized on a CM5 sensor chip (BIAcore) through amine coupling. The carboxylic acid groups of a dextran matrix were activated with 70 μL (10 μL/min) of a mixture of 0.2 M EDC and 0.05 M NHS (*N*-hydroxysuccinimide). The complex was injected over the course of 7 min (10 μL/min), resulting in approximately 18000 resonance units of immobilized protein, and the reaction was stopped by the injection of 70 μL (10 μL/min) of 1 M ethanolamine hydrochloride in order to transform the remaining active esters into amides. This procedure allows the Tmc complex to be covalently bound to the carboxymethyl dextran-modified gold surface via the exposed amino groups. The continuous flow cell was equilibrated with the running buffer that contains 10 mM HEPES (pH 7.4), 150 mM NaCl, 3 mM EDTA, and 0.005% P20. TpIc_3, APS reductase, and sulfite reductase were diluted in running buffer and injected using a constant flow rate of 10 μL/min (30 μL). The resulting sensorgrams were evaluated using the biomolecular interaction analysis evaluation software (BIAcore) in order to calculate the kinetic constants of the complex formation.

RESULTS

None of the *Desulfovibrio* membrane-bound electron transfer complexes associated with a cytochrome of the cytochrome c_3 family had been isolated thus far. With the aim to study the function of these complexes in the respiratory chain of *Desulfovibrio* spp., we decided to attempt isolation of the Tmc complex in *D. vulgaris*, since it shows higher levels of expression than the Hmc complex (*30*) and also has a simpler subunit composition. For this process it is first essential to conduct a thorough analysis of the sequences predicted by genes of the Tmc gene cluster.

Desulfovibrio TmcABCD-Encoded Proteins. The gene cluster coding for the Tmc complex is present in the genomes of *D. vulgaris* Hildenborough and *D. desulfuricans* G20, where it is identical, but is not found in *Dt. psycrophila* or *A. fulgidus*. This gene cluster includes nine genes (DVU0258−DVU0266, Figure 1) and is predicted to form an operon (*31*). Gene DVU0258 is predicted to encode a signal transduction histidine kinase; genes DVU0259 and DVU0260 are both predicted to encode DNA-binding response regulators, and DVU0261 is also predicted to code for a DNA-binding universal stress protein.

Thus, genes DVU0258−DVU0261 are all likely to be involved in regulation of the Tmc expression. Gene DVU0262 encodes for a hypothetical protein, and DVU0263 encodes for TmcA, the periplasmic tetraheme TpIIc_3 that was previously characterized (*22*). DVU0264 encodes for a hydrophilic protein, named as TmcB, predicted to be cytoplasmic due to the lack of a signal peptide. TmcB is

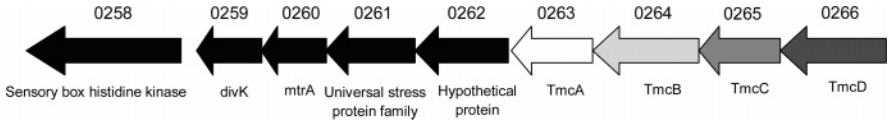

FIGURE 1: Schematic representation of the genes enconding the Tmc complex in *Desulfovibrio*. The genes represented correspond to DVU0258−DVU0266 of *D. vulgaris* Hildenborough and Dde3715−3707 of *D. desulfuricans* G20.

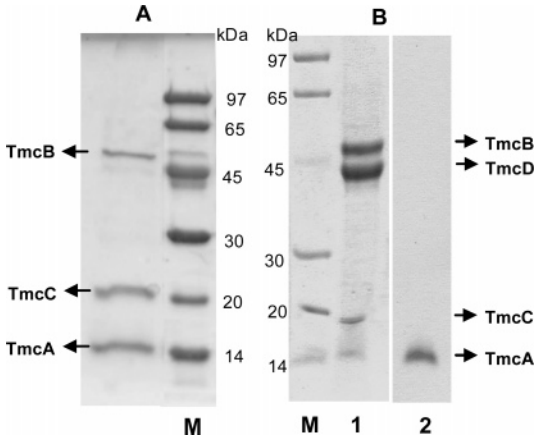

FIGURE 2: SDS−PAGE of the Tmc complex from *D. vulgaris* Hildenborough. (A) Basic fraction containing the truncated form of the complex. (B) Acidic fraction containing the $TmcA_2BCD$ complex, stained with Coomassie Blue (1) and heme staining (2). Lanes M are the molecular mass markers.

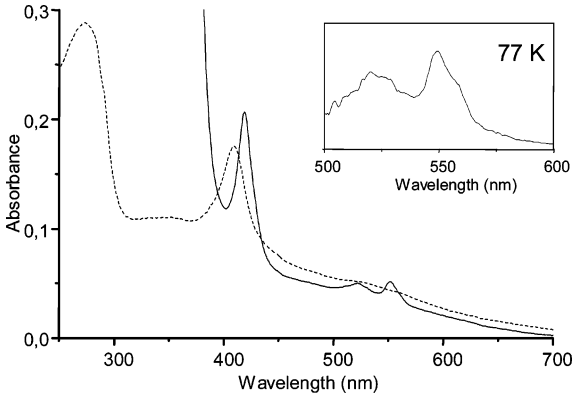

FIGURE 3: UV−visible spectra of the Tmc complex at room temperature and at 77 K (inset): dashed line, as-isolated oxidized protein; solid line, reduced with dithionite.

closely related to the HmcF subunit of the *D. vulgaris* Hmc complex, with which it shares 31% identity and 50% similarity. Both TmcB and HmcF belong to a very interesting family of FeS proteins that also includes DsrK, the cytoplasmic subunit of the Dsr complex, and of which the best studied member is HdrD, the catalytic subunit of membrane-bound heterodisulfide reductases (Hdr) of methanogens (*32*). Numerous proteins belonging to this family are found in protein databases and the genomes of many organisms, although their function is unknown. They are usually associated with membrane-bound and redox cofactor-containing subunits, indicating that they are involved in respiratory electron transfer chains. Thus, TmcB is a representative of a whole family of widespread proteins of which not much is known to date. All proteins in this family have two $[4Fe4S]^{2+/1+}$ binding sites at the N-terminus and one or two conserved five-cysteine motifs $CX_nCCX_nCX_2C$. In HdrD some of these cysteines are involved in binding an unusual $[4Fe4S]^{3+}$ center that is the catalytic site of the heterodisulfide reduction (*33*). DVU0265 encodes for an integral membrane protein, named as TmcC, that belongs to the family of heme *b*-containing subunits of respiratory oxidoreductases. It is homologous to the HmcE subunit of the Hmc complex (32% identity and 50% similarity) and is predicted to contain four transmembrane helices. TmcC and HmcE of *D. vulgaris* and *D. desulfuricans* G20 share four conserved histidines that are likely candidates to bind two hemes *b*, and two of them align with the histidines that are the ligands to the hemes *b* in *Escherichia coli* NarI (*34*). DVU0266 encodes for a protein named as TmcD that shows no similarity to any proteins in the databases, except the homologous protein in *D. desulfuricans* G20. The start of its N-terminal sequence is not correctly predicted in the genome (see below). It has no transmembrane helices or signal peptide, but a conspicuously high number of tryptophan residues (22 in 418 amino acids, 5.3%). Tryptophan is a preferred amino acid found in the regions of membrane proteins that are close to the membrane−water interface (*35*). Its hydrophobic, yet polar, aromatic ring is particularly suited for interacting with the polar−apolar border. TmcD is thus likely to be a peripheral membrane protein of the Tmc complex.

Purification and Biochemical Characterization of the Tmc Complex. The cytochrome *c* subunit of the Tmc complex, the $TpIIc_3$, has previously been isolated using a strong detergent, which probably causes it to dissociate from the complex (*22*). To try to isolate the whole complex, we extracted the membrane fraction of *D. vulgaris* using a mild detergent to avoid separation of the subunits. After purification of the detergent extract on two consecutive Q-Sepharose columns, two fractions were identified that displayed UV−visible absorption for both *b*- and *c*-type hemes and also a 14 kDa band on SDS gel electrophoresis that stained positive for heme *c*. The first fraction was more basic and eluted at 100 mM NaCl, whereas the second fraction was very acidic and eluted only at 1 M NaCl. The fraction eluted at 100 mM NaCl displayed two bands on a SDS gel with apparent molecular masses of 14 and 20 kDa and a weak band at 50 kDa (Figure 2A).

N-Terminal sequences were obtained for the 14 and 50 kDa bands, whereas the 20 kDa band gave no sequence possibly because of a blocked N-terminus. The two sequences obtained enabled identification of the corresponding genes as DVU0263 (14 kDa band; TmcA) and DVU0265 (50 kDa band; TmcB), which are both part of the predicted *tmc* operon. The more acidic fraction displayed also the two bands at 14 and 20 kDa, but weaker, and two strong bands at 45 and 50 kDa (Figure 2B). The N-terminal sequence of the 50 kDa band in this fraction confirms that it also corresponds to the TmcB protein. The N-terminal sequence obtained for the 45 kDa band was MRSPTAW, which revealed that this band corresponds to the hypothetical protein in the *tmc* operon predicted by gene DVU0266 but that the start of the N-terminal sequence is not correctly predicted in the genome. Since both fractions display visible absorption

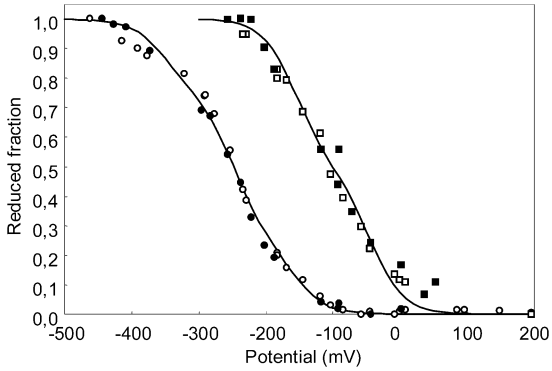

FIGURE 4: Redox titration of the Tmc hemes followed by visible spectroscopy. The points represent the oxidation (●) and reduction (○) at 552 nm (dominated by the contribution of the hemes *c*) and the oxidation (■) and reduction (□) at 561 nm (dominated by the contribution of the hemes *b*) of Tmc following changes at the α-band. The solid line corresponds to a theoretical simulation obtained by adding four Nernst equations with redox potentials of −160, −245, −250, and −350 mV, considering equal optical contribution for all hemes *c*, and two Nernst equations for hemes *b* with redox potentials of −155 and −45 mV in a 1:1 ratio.

corresponding to the presence of hemes *b*, it is likely that the 20 kDa band corresponds to the TmcC protein.

A densitometric analysis of the bands in the more acidic fraction yielded the following ratio for the four subunits: 50 kDa:45 kDa:20 kDa:14 kDa = 1:1.3:1.1:2.1, suggesting that this fraction corresponds to a native form of the Tmc complex with an $\alpha_2\beta\gamma\delta$ composition of the TmcA, TmcB, TmcC, and TmcD subunits (TmcA$_2$BCD). The less acidic fraction seems to correspond to a truncated version of the complex (TmcAC) that contains mainly the two heme proteins TmcA and TmcC (and very little of the TmcB protein), indicating that TmcB and TmcD can dissociate from the other two subunits and possibly have a weaker interaction with the membranes.

UV−Visible Spectroscopy. The *D. vulgaris* Tmc complex has a strong absorbance in the visible region in agreement with a protein containing several hemes and FeS centers (Figure 3). At room temperature, the as-isolated oxidized complex has a heme Soret peak with a maximum at 409 nm. In the reduced state, the Soret peak shifts to 419 nm and the heme α and β peaks are observed at 551.5 and 522 nm, respectively. At room temperature, the heme α-band of the reduced complex presents a small shoulder at higher wavelengths, probably due to the hemes *b*. When the spectrum is run at liquid nitrogen temperature, this shoulder is more pronounced, supporting the presence of the two distinct types of hemes, as the shoulder is not observed in the low-temperature spectrum of the isolated TpIIc_3.

Sequence analysis of the Tmc complex predicts the presence of four hemes *c* in TmcA and two hemes *b* in TmcC. We estimated the concentration of hemes *b* and *c* in the Tmc complex using the method described by Berry and Trumpower (*26*) and observed a ratio of five hemes *c per* heme *b*, which agrees with the presence of two TmcA subunits and one TmcC subunit in the complex. A similar ratio was observed for the TmcAC fraction.

Measuring the absorbance changes at 552 and 561 nm in redox titrations followed by visible spectroscopy, it is possible to obtain curves that are dominated by the titration of *c*-type and *b*-type hemes, respectively. The data obtained in the α-band region are corroborated by data measured in the Soret region (data not shown). The hemes *c* start to be reduced at ∼ −100 mV and are fully reduced at ∼ −500 mV, and the hemes *b* start at ∼ +50 mV and are fully reduced at ∼ −200 mV (Figure 4). The experimental data could be simulated by adding a minimum of four Nernst equations with redox potentials of −160, −245, −250, and −350 mV for the hemes *c* and two Nernst equations for the hemes *b* with redox potentials of −155 and −45 mV in a 1:1 ratio. These simulations considered an equal optical contribution for all hemes and that no interactions were present. Comparison of the redox potentials of the hemes *c* in isolated TpIIc_3 (−170, −235, −260, and −325 mV) (*22*) and in the Tmc complex shows only small differences between them.

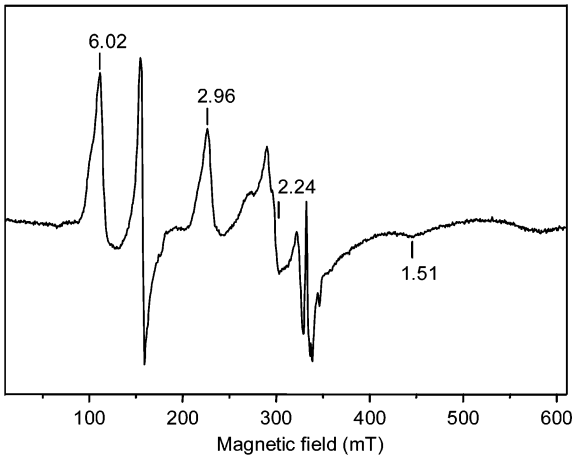

FIGURE 5: EPR spectrum of the as-prepared oxidized Tmc complex from *Dv*H at 10 K. Experimental conditions: microwave frequency, 9.64 GHz; microwave power, 2.4 mW; modulation frequency, 100 kHz; modulation amplitude, 1 mT.

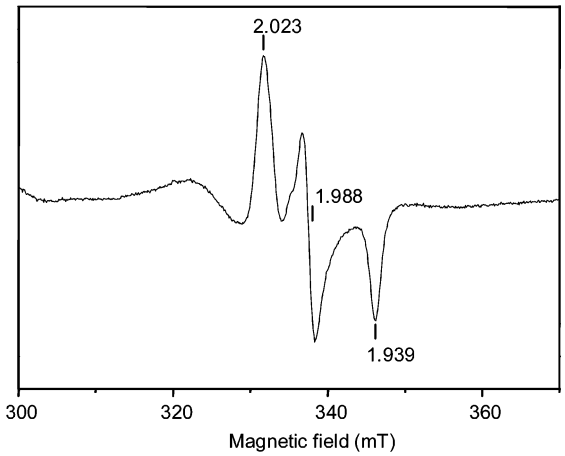

FIGURE 6: EPR spectrum of the rhombic signal in the oxidized Tmc complex at 17 K. Experimental conditions: microwave frequency, 9.64 GHz; microwave power, 2.4 mW; modulation frequency, 100 kHz; modulation amplitude, 1 mT.

EPR Spectroscopy. The low-temperature EPR spectrum of the as-prepared oxidized Tmc complex shows features typical of low-spin ferric hemes with $g_{max} = 2.96$, $g_{med} \sim 2.24$, and $g_{min} = 1.51$ (Figure 5). A signal with $g_{max} = 6.02$ is also observed that probably corresponds to a heme in the high-spin state. The intensity of this signal is about 10% of the $g_{max} = 2.96$ signal, suggesting that one heme (in the total of 10) in the complex may be five coordinated.

As expected from sequence analysis, a rhombic signal with $g_{max} = 2.023$, $g_{med} = 1.998$, and $g_{min} = 1.939$ is also present,

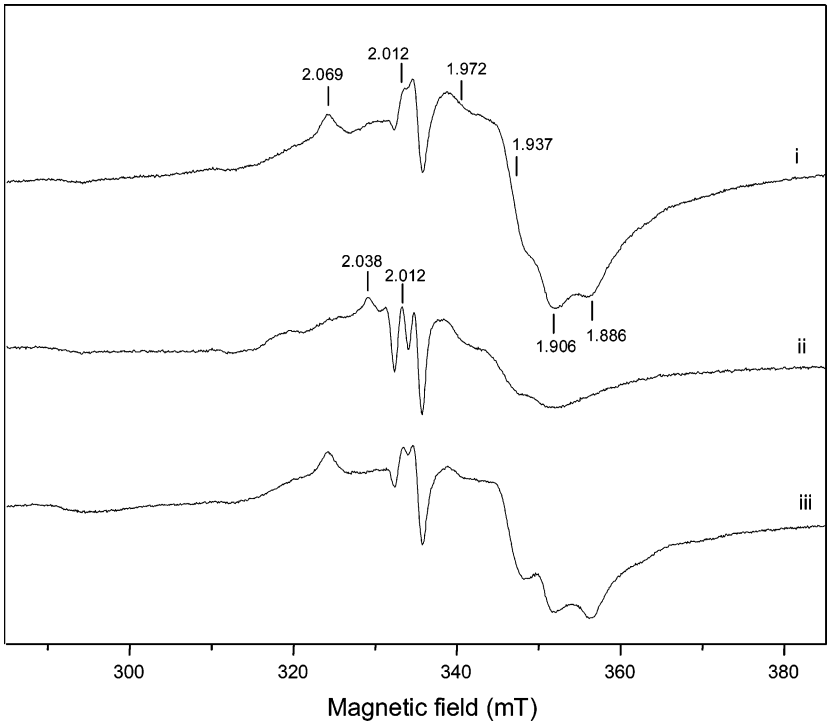

FIGURE 7: EPR spectra of the reduced Tmc complex: (i) reduced with dithionite, 10 K, (ii) reduced with dithionite, 20 K, and (iii) reduced with H_2 and 0.6 μM [NiFeSe] hydrogenase/0.6 μM TpIc_3, 10 K.

observed with maximum intensity at 17 K (Figure 6). This characteristic signal is also present in the Dsr complex from *D. desulfuricans* (*9*) and *A. fulgidus* (*10*) and also in Hdr after binding of a thiol substrate (*36*). In Hdrs it has been shown that this signal is due to a $[4Fe4S]^{3+}$ cluster that is the catalytic site of the enzyme (*33*, *36*−*38*). As observed for the Dsr complexes, this signal is detected in Tmc in the oxidized native state without addition of any exogenous substrate, indicating the presence of a similar $[4Fe4S]^{3+}$ center in the TmcB subunit. This signal titrates with a redox potential of +115 mV, which is close to the redox potential observed for the Dsr complex (+130 mV).

Upon reduction of Tmc with dithionite a complex signal is observed indicative of the presence of $[4Fe4S]^{+}$ centers (Figure 7, i and ii). The sequence of TmcB includes two canonical binding sites for $[4Fe4S]^{2+/1+}$ centers. However, the signal observed seems to be too complex to be caused by only two such centers, even if magnetic interactions are likely to exist. The EPR spectrum suggests that a fourth FeS center may be present in TmcB. There are seven cysteines (apart from the eight of the two canonical $[4Fe4S]^{2+/1+}$ binding sites), one histidine, and one aspartate conserved in TmcB and related proteins. Four of these cysteines are likely to be involved in the binding of the $[4Fe4S]^{3+/2+}$ center, but this still leaves enough conserved residues to account for a third center of the $[4Fe4S]^{2+/1+}$ or $[2Fe4S]^{2+/1+}$ type. A signal due to a radical species ($g = 2.00$) of unknown origin may also be present in the reduced EPR spectrum. No signals were detected at temperatures above 60 K.

Functional Analysis of the Tmc Complex. The structural arrangement of the Tmc complex suggests that it may interact with redox partners in the periplasm (through the cytochrome *c* subunit, TmcA), with the membrane-associated menaquinone pool (through the TmcC subunit), or with redox partners in the cytoplasm (through the FeS subunit, TmcB). It has been shown that TpIIc_3, the cytochrome *c* subunit of Tmc, is reduced by periplasmic-facing hydrogenases with the TpIc_3 as mediator (*22*, *39*), suggesting that the Tmc complex is a receptor for electrons resulting from periplasmic hydrogen oxidation. To evaluate whether electrons can flow from the TmcA subunit to the cytoplasmic TmcB subunit, we ran an EPR spectrum of the Tmc complex reduced with hydrogen by catalytic amounts of *D. vulgaris* [NiFeSe] hydrogenase and TpIc_3. The spectrum shows complete reduction of all of the hemes and of the rhombic signal and also almost complete reduction of the FeS centers of the TmcB subunit (Figure 7, iii), indicating that indeed electrons can flow through the complex to the cytoplasmic subunit. The interaction between the Tmc complex and TpIc_3 was also analyzed by surface plasmon resonance (Biacore), whereby the Tmc complex was immobilized in a CM5 sensor chip. A specific interaction between the two proteins was observed (Figure 8), but the high level of unspecific interaction between TpIc_3 and the activated−deactivated matrix of the control channel precluded us from calculating kinetic constants for association/dissociation (the values that would be obtained would have no real physical meaning).

We also tested the possibility of electron transfer between the Tmc complex and menaquinone. For this, the complex was reduced using *D. vulgaris* hydrogenases and then incubated with the menaquinone analogue DMN, and this resulted in reduction of DMN. However, when this experiment was repeated with the isolated TmcA subunit at the same concentration, a similar reduction rate of DMN was observed, suggesting that the membrane subunit TmcC is not involved in the quinone reduction. Reduced TpIc_3 could also efficiently transfer electrons to DMN. This reduction is probably the result of a nonspecific electron transfer driven by the difference in redox potential between the cytochromes *c* and menaquinones and may have no biological significance.

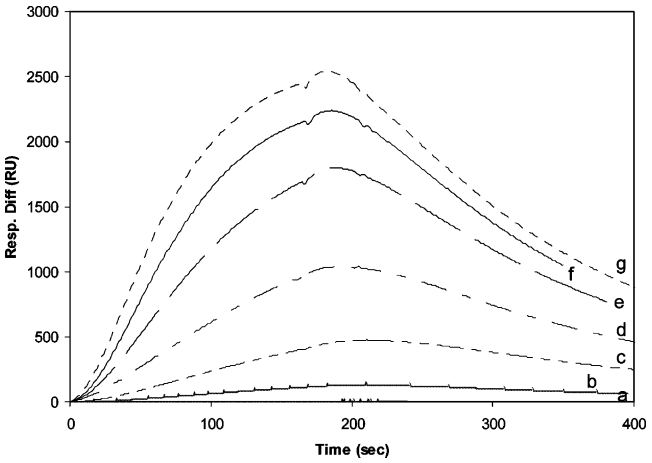

FIGURE 8: Concentration dependence curves for binding of TpIc_3 to the Tmc complex immobilized onto a CM5 sensor chip, analyzed by surface plasmon resonance. The sensorgrams are the subtraction of the response for the Tmc immobilized channel minus the control channel (activated−deactivated matrix). TpIc_3 was injected at concentrations of 0 nM (a), 50 nM (b), 200 nM (c), 400 nM (d), 600 nM (e), 800 nM (f), and 1000 nM (g) at a flow rate of 10 μL/min for 3 min at 25 °C. The sensorgrams show binding of TpIc_3 to the immobilized Tmc complex during the injection, followed by cytochrome dissociation from the receptor surface after injection stops.

Nevertheless, it is interesting to consider the possibility of direct electron transfer between the abundant cytochrome c_3 pool and the menaquinone pool, since it is known that some of the TpIc_3 is found to be membrane associated (*22*). We tested also the reduction of the Tmc complex by borohydride-reduced DMN inside the anaerobic chamber. No reduction of the hemes could be observed, which is in agreement with the redox potentials determined for the complex and the higher redox potential of DMN (−60 mV). These results suggest that the hemes *b* of the Tmc complex are not involved in electron transfer with the menaquinone/menaquinol pool in the membrane, and thus their role is likely to be as a conduit for electrons from the TmcA subunit to the TmcB subunit.

The cytoplasmic TmcB subunit is likely to fuel electrons to the sulfate reduction pathway. We tested whether a direct interaction between the Tmc complex and some enzymes involved in the sulfate reduction pathway could occur. Initially, cross-linking reactions between the Tmc complex (in oxidized and reduced forms) and APS reductase and sulfite reductase of *D. vulgaris* were carried out. No conclusions could be obtained from these experiments because the complex aggregates in the presence of EDC and does not run in SDS−PAGE. Surface plasmon resonance analysis of the interaction between the immobilized Tmc complex and APS reductase and sulfite reductase was performed. No specific interaction could be detected under the conditions used.

DISCUSSION

In this study we report the isolation and characterization of the Tmc complex from *D. vulgaris*, a transmembrane complex proposed to be involved in the sulfate respiratory pathway. The Tmc complex was isolated from the membranes of *D. vulgaris* displaying four subunits in a SDS gel, with molecular masses of 14, 20, 45, and 50 kDa. The 14 kDa subunit was identified as TpIIc_3 (TmcA) by heme staining and N-terminal sequence. The 50 and 45 kDa bands were identified by N-terminal sequence as the TmcB and TmcD subunits, respectively. The 20 kDa band was not identified by N-terminal sequence, but the detection of hemes *b* by UV−visible spectroscopy indicates that it corresponds to the TmcC subunit. The evidence obtained suggests that the isolated Tmc complex has a TmcA$_2$BCD composition. A truncated form of the complex constituted mainly by TmcA and TmcC was also obtained, suggesting a weaker interaction with the TmcB and TmcD subunits. The genes enconding these proteins are part of a nine-gene cluster predicted to form an operon (*31*). Downstream of the TmcA gene there are three genes coding for three response regulators (DVU258, divK, and mtrA) and one gene coding for a protein that belongs to a universal stress protein family. This suggests an intricate regulation of the Tmc complex expression.

Molecular hydrogen plays a central role in the metabolism of sulfate-reducing bacteria (*3*). The couple hydrogenase/TpIc_3 is the key system for hydrogen oxidation in *Desulfovibrio*. The two components work together, hydrogenase catalyzing the splitting or the synthesis of molecular hydrogen and TpIc_3 acting as the electron and proton transport protein (*40*). *Desulfovibrio* spp. contain some membrane-bound electron transfer complexes (Hmc, Tmc, and 9Hc) that are not found in other sulfate reducers such as *Dt. psychrophila* or *A. fulgidus* and which include a periplasmic cytochrome *c* subunit of the cytochrome c_3 family (*3*). The other subunits of these complexes also show a high degree of sequence similarity between them indicating their homology. The larger Hmc complex shows a striking similarity in subunit composition to the Dsr complex conserved in all sulfate reducers, but the actual sequence similarity between subunits is quite low (*9*). Functional studies of these *Desulfovibrio* complexes have been mostly performed with Hmc and indicate its role in transmembrane electron transfer when hydrogen is the electron donor for growth (*16*−*18*). Several studies have also shown that TpIIc_3, the periplasmic subunit of the Tmc complex, accepts electrons from TpIc_3 (*22*, *41*−*43*), suggesting that the Tmc complex may have a similar function to Hmc in accepting electrons from hydrogen oxidation. Our results showing that nearly full reduction of the Tmc complex can be attained in the presence of hydrogenase/TpIc_3 are a strong evidence in favor of this hypothesis. In proteomic studies, we also observed that *D. vulgaris* cells grown with hydrogen as sole energy source have increased amounts of TpIIc_3 (unpublished results), further substantiating the role of Tmc in hydrogen metabolism. Although the structure of the Tmc complex is unknown at present, the arrangement of the subunits relative to the membrane shows a gradient in the reduction potentials of the cofactors with increasing potentials from the periplasmic to cytoplasmic side. This downhill pathway may serve to commit the electrons to this route of entry into the cytoplasm. In terms of subunit composition, the Tmc complex is a simplified version of the larger Hmc complex. During purification of the Tmc complex no Hmc complex or HmcA could be detected. It is thus tempting to suggest that the Tmc complex may substitute for Hmc and that, for some reason not fully understood, the conditions used here to grow the cells induced expression of Tmc and repressed Hmc. Further

work will be necessary to evaluate whether regulation of Hmc and Tmc expression is linked.

The isolation of the simpler Tmc complex permitted an analysis of some of its subunits that would be more difficult to carry out with Hmc. For example, the evidence shown here suggests that the role of the cytochrome *b* subunit, TmcC, is in electron transfer between TmcA and TmcB and probably not in electron transfer with the quinone pool, although this cannot be ruled out. The FeS clusters of the TmcB subunit could also be analyzed without the confounding presence of other FeS proteins. We observed the characteristic EPR signal in the oxidized Tmc complex that is attributed to the $[4Fe4S]^{3+}$ cluster, observed also in Hdr and the Dsr complex, which confirms the sequence-predicted similarity between TmcB, DsrK, and HdrD. In addition, EPR analysis suggests that TmcB may include another FeS center not predicted by sequence analysis. The precise function of this cytoplasmic subunit present in the Tmc, Hmc, and Dsr complexes remains unknown, but it is likely to be involved in the electron transfer for the cytoplasmic sulfate reduction. We could not observe a direct interaction between the Tmc complex and APS reductase or sulfite reductase, suggesting the involvement of other proteins or cofactors. A likely possibility, discussed before (*9*), is the involvement of a thiol/disulfide in this process due to the similarities to HdrD. The Tmc complex also includes one subunit (TmcD) that is not present in Hmc or any other complex and shows no relationship to any protein in the databases. The function of this protein is presently unknown. It is not predicted to contain cofactors but includes an unusually high number of tryptophans which may be involved in membrane binding.

In conclusion, a novel membrane-bound redox complex was isolated and characterized from the sulfate-reducing bacterium *D. vulgaris* Hildenborough. The evidence obtained indicates that this complex is involved in transferring electrons from the periplasmic oxidation of hydrogen to a still unidentified electron acceptor involved in sulfate reduction. Further studies are necessary to clarify the important role of the transmembrane complexes in the sulfate respiratory pathway.

ACKNOWLEDGMENT

The authors thank João Carita (ITQB) for growing the bacterial cells and Manuela Regalla (ITQB) for amino acid sequencing.

REFERENCES

1. Rabus, R., Hansen, T., and Widdel, F. (2000) Dissimilatory Sulfate- and Sulfur-Reducing Prokaryotes, in *The Prokaryotes: An Evolving Electronic Resource for the Microbiological Community* (Dworkin, M. E. A., Ed.) Springer-Verlag (http://link-.springer-ny.com/link/service/books/10125/), New York.
2. Jørgensen, B. B. (1982) Mineralization of organic matter in the sea-bed—the role of sulphate reduction, *Nature 390*, 364−370.
3. Matias, P. M., Pereira, I. A. C., Soares, C. M., and Carrondo, M. A. (2005) Sulphate respiration from hydrogen in *Desulfovibrio* bacteria: a structural biology overview, *Prog. Biophys. Mol. Biol. 89*, 292−329.
4. Heidelberg, J. F., Seshadri, R., Haveman, S. A., Hemme, C. L., Paulsen, I. T., Kolonay, J. F., Eisen, J. A., Ward, N., Methe, B., Brinkac, L. M., Daugherty, S. C., Deboy, R. T., Dodson, R. J., Durkin, A. S., Madupu, R., Nelson, W. C., Sullivan, S. A., Fouts, D., Haft, D. H., Selengut, J., Peterson, J. D., Davidsen, T. M., Zafar, N., Zhou, L. W., Radune, D., Dimitrov, G., Hance, M., Tran, K., Khouri, H., Gill, J., Utterback, T. R., Feldblyum, T. V., Wall, J. D., Voordouw, G., and Fraser, C. M. (2004) The genome sequence of the anaerobic, sulfate-reducing bacterium *Desulfovibrio vulgaris* Hildenborough, *Nat. Biotechnol. 22*, 554−559.
5. Rabus, R., Ruepp, A., Frickey, T., Rattei, T., Fartmann, B., Stark, M., Bauer, M., Zibat, A., Lombardot, T., Becker, I., Amann, J., Gellner, K., Teeling, H., Leuschner, W. D., Glockner, F. O., Lupas, A. N., Amann, R., and Klenk, H. P. (2004) The genome of *Desulfotalea psychrophila*, a sulfate-reducing bacterium from permanently cold Arctic sediments, *Environ. Microbiol. 6*, 887−902.
6. Klenk, H. P., Clayton, R. A., Tomb, J. F., White, O., Nelson, K. E., Ketchum, K. A., Dodson, R. J., Gwinn, M., Hickey, E. K., Peterson, J. D., Richardson, D. L., Kerlavage, A. R., Graham, D. E., Kyrpides, N. C., Fleischmann, R. D., Quackenbush, J., Lee, N. H., Sutton, G. G., Gill, S., Kirkness, E. F., Dougherty, B. A., McKenney, K., Adams, M. D., Loftus, B., Venter, J. C., et al. (1997) The complete genome sequence of the hyperthermophilic, sulphate-reducing archaeon *Archaeoglobus fulgidus*, *Nature 390*, 364−370.
7. Pires, R. H., Lourenco, A. I., Morais, F., Teixeira, M., Xavier, A. V., Saraiva, L. M., and Pereira, I. A. (2003) A novel membrane-bound respiratory complex from *Desulfovibrio desulfuricans* ATCC 27774, *Biochim. Biophys. Acta 1605*, 67−82.
8. Haveman, S. A., Greene, E. A., Stilwell, C. P., Voordouw, J. K., and Voordouw, G. (2004) Physiological and gene expression analysis of inhibition of *Desulfovibrio vulgaris* Hildenborough by nitrite, *J. Bacteriol. 186*, 7944−7950.
9. Pires, R. H., Venceslau, S. S., Morais, F., Teixeira, M., Xavier, A. V., and Pereira, I. A. C. (2006) Characterization of the *Desulfovibrio desulfuricans* ATCC 27774 DsrMKJOP complex—a membrane-bound redox complex involved in sulfate respiration, *Biochemistry 45*, 249−262.
10. Mander, G. J., Duin, E. C., Linder, D., Stetter, K. O., and Hedderich, R. (2002) Purification and characterization of a membrane-bound enzyme complex from the sulfate-reducing archaeon *Archaeoglobus fulgidus* related to heterodisulfide reductase from methanogenic archaea, *Eur. J. Biochem. 269*, 1895−1904.
11. Mussmann, M., Richter, M., Lombardot, T., Meyerdierks, A., Kuever, J., Kube, M., Glockner, F. O., and Amann, R. (2005) Clustered genes related to sulfate respiration in uncultured prokaryotes support the theory of their concomitant horizontal transfer, *J. Bacteriol. 187*, 7126−7137.
12. Pereira, I. A. C., and Xavier, A. V. (2005) Multi-Heme *c* Cytochromes and Enzymes, in *Encyclopedia of Inorganic Chemistry* (King, R. B., Ed.) John Wiley & Sons, New York.
13. Rossi, M., Pollock, W. B., Reij, M. W., Keon, R. G., Fu, R., and Voordouw, G. (1993) The hmc operon of *Desulfovibrio vulgaris* subsp. *vulgaris* Hildenborough encodes a potential transmembrane redox protein complex, *J. Bacteriol. 175*, 4699−4711.
14. Matias, P. M., Coelho, A. V., Valente, F. M. A., D., P., LeGall, J., Xavier, A. V., Pereira, I. A. C., and Carrondo, M. A. (2002) Sulfate respiration in *Desulfovibrio vulgaris* Hildenborough: Structure of the 16-heme cytochrome *c* HmcA at 2.5 Å resolution and a view of its role in transmembrane electron transfer, *J. Biol. Chem. 277*, 47907−47916.
15. Czjzek, M., ElAntak, L., Zamboni, V., Morelli, X., Dolla, A., Guerlesquin, F., and Bruschi, M. (2002) The crystal structure of the hexadeca-heme cytochrome Hmc and a structural model of its complex with cytochrome c_3, *Structure 10*, 1677−1686.
16. Keon, R. G., Fu, R., and Voordouw, G. (1997) Deletion of two downstream genes alters expression of the hmc operon of *Desulfovibrio vulgaris* subsp. *vulgaris* Hildenborough, *Arch. Microbiol. 167*, 376−383.
17. Dolla, A., Pohorelic, B. K. J., Voordouw, J. K., and Voordouw, G. (2000) Deletion of the hmc operon of *Desulfovibrio vulgaris* subsp. *vulgaris* Hildenborough hampers hydrogen metabolism and low-redox-potential niche establishment, *Arch. Microbiol. 174*, 143−151.
18. Voordouw, G. (2002) Carbon monoxide cycling by *Desulfovibrio vulgaris* Hildenborough, *J. Bacteriol. 184*, 5903−5911.
19. Pereira, I. A. C., Romão, C. V., Xavier, A. V., LeGall, J., and Teixeira, M. (1998) Electron transfer between hydrogenases and mono and multiheme cytochromes in *Desulfovibrio spp.*, *J. Biol. Inorg. Chem. 3*, 494−498.
20. Saraiva, L. M., da Costa, P. N., Conte, C., Xavier, A. V., and LeGall, J. (2001) In the facultative sulphate/nitrate reducer *Desulfovibrio desulfuricans* ATCC 27774, the nine-haem cyto-

chrome *c* is part of a membrane-bound redox complex mainly expressed in sulphate-grown cells, *Biochim. Biophys. Acta 1520*, 63−70.
21. Matias, P. M., Coelho, R., Pereira, I. A., Coelho, A. V., Thompson, A. W., Sieker, L. C., Gall, J. L., and Carrondo, M. A. (1999) The primary and three-dimensional structures of a nine-haem cytochrome *c* from *Desulfovibrio desulfuricans* ATCC 27774 reveal a new member of the Hmc family, *Structure 7*, 119−130.
22. Valente, F. M. A., Saraiva, L. M., LeGall, J., Xavier, A. V., Teixeira, M., and Pereira, I. A. C. (2001) A membrane-bound cytochrome c_3: A type II cytochrome c_3 from *Desulfovibrio vulgaris* Hildenborough, *ChemBioChem 2*, 895−905.
23. Pereira, P. M., Pacheco, I., Turner, D. L., and Louro, R. O. (2002) Structure−function relationship in type II cytochrome c_3 from *Desulfovibrio africanus*: a novel function in a familiar heme core, *J. Biol. Inorg. Chem. 7*, 815−822.
24. Huynh, B. H., Czechowski, M. H., Kruger, H. J., Dervartanian, D. V., Peck, H. D., and Legall, J. (1984) *Desulfovibrio vulgaris* hydrogenase—a nonheme iron enzyme lacking nickel that exhibits anomalous electron-paramagnetic-resonance and Mossbauer-spectra, *Proc. Natl. Acad. Sci. U.S.A. 81*, 3728−3732.
25. Schägger, H. (1994) *A Practical Guide to Membrane Protein Purification* (Jagow, H. S. E. G. V., Ed.) Academic Press, San Diego, CA.
26. Berry, E. A., and Trumpower, B. L. (1987) Simultaneous determination of hemes *a*, *b*, and *c* from pyridine hemochrome spectra, *Anal. Biochem. 161*, 1−15.
27. Teixeira, M., Campos, A. P., Aguiar, A. P., Costa, H. S., Santos, H., Turner, D. L., and Xavier, A. V. (1993) Pitfalls in assigning heme axial coordination by EPR. *c*-Type cytochromes with atypical Met-His ligation, *FEBS Lett. 317*, 233−236.
28. Lemma, E., Unden, G., and Kroger, A. (1990) Menaquinone is an obligatory component of the chain catalyzing succinate respiration in *Bacillus subtilis*, *Arch. Microbiol. 155*, 62−67.
29. Snyder, C. H., and Trumpower, B. L. (1999) Ubiquinone at center N is responsible for triphasic reduction of cytochrome *b* in the cytochrome *bc*(1) complex, *J. Biol. Chem. 274*, 31209−31216.
30. Haveman, S. A., Brunelle, V., Voordouw, J. K., Voordouw, G., Heidelberg, J. F., and Rabus, R. (2003) Gene expression analysis of energy metabolism mutants of *Desulfovibrio vulgaris* Hildenborough indicates an important role for alcohol dehydrogenase, *J. Bacteriol. 185*, 4345−4353.
31. Price, M. N., Huang, K. H., Alm, E. J., and Arkin, A. P. (2005) A novel method for accurate operon predictions in all sequenced prokaryotes, *Nucleic Acids Res. 33*, 880−892.
32. Kunkel, A., Vaupel, M., Heim, S., Thauer, R. K., and Hedderich, R. (1997) Heterodisulfide reductase from methanol-grown cells of *Methanosarcina barkeri* is not a flavoenzyme, *Eur. J. Biochem. 244*, 226−234.
33. Duin, E. C., Bauer, C., Jaun, B., and Hedderich, R. (2003) Coenzyme M binds to a [4Fe-4S] cluster in the active site of heterodisulfide reductase as deduced from EPR studies with the [33S]coenzyme M-treated enzyme, *FEBS Lett. 538*, 81−84.
34. Bertero, M. G., Rothery, R. A., Palak, M., Hou, C., Lim, D., Blasco, F., Weiner, J. H., and Strynadka, N. C. (2003) Insights into the respiratory electron transfer pathway from the structure of nitrate reductase A, *Nat. Struct. Biol. 10*, 681−687.
35. Killian, J. A., and von Heijne, G. (2000) How proteins adapt to a membrane-water interface, *Trends Biochem. Sci. 25*, 429−434.
36. Duin, E. C., Madadi-Kahkesh, S., Hedderich, R., Clay, M. D., and Johnson, M. K. (2002) Heterodisulfide reductase from *Methanothermobacter marburgensis* contains an active-site [4Fe-4S] cluster that is directly involved in mediating heterodisulfide reduction, *FEBS Lett. 512*, 263−268.
37. Bennati, M., Weiden, N., Dinse, K. P., and Hedderich, R. (2004) (57)Fe ENDOR spectroscopy on the iron-sulfur cluster involved in substrate reduction of heterodisulfide reductase, *J. Am. Chem. Soc. 126*, 8378−8379.
38. Shokes, J. E., Duin, E. C., Bauer, C., Jaun, B., Hedderich, R., Koch, J., and Scott, R. A. (2005) Direct interaction of coenzyme M with the active-site Fe-S cluster of heterodisulfide reductase, *FEBS Lett. 579*, 1741−1744.
39. Valente, F. M. A., Oliveira, A. S. F., Gnadt, N., Pacheco, I., Coelho, A. V., Xavier, A. V., Teixeira, M., Soares, C. M., and Pereira, I. A. C. (2005) Hydrogenases in *Desulfovibrio vulgaris* Hildenborough: structural and physiologic characterisation of the membrane-bound [NiFeSe] hydrogenase, *J. Biol. Inorg. Chem. 10*, 667−682.
40. Louro, R. O., Catarino, T., LeGall, J., and Xavier, A. V. (1997) Redox-Bohr effect in electron/proton energy transduction: cytochrome c_3 coupled to hydrogenase works as a "proton thruster" in *Desulfovibrio vulgaris*, *J. Biol. Inorg. Chem. 2*, 488−491.
41. Magro, V., Pieulle, L., Forget, N., Guigliarelli, B., Petillot, Y., and Hatchikian, E. C. (1997) Further characterization of the two tetraheme cytochromes c_3 from *Desulfovibiro africanus*: nucleotide sequences, EPR spectroscopy and biological activity, *Biochim. Biophys. Acta 1342*, 149−163.
42. Teixeira, V. H., Baptista, A. M., and Soares, C. M. (2004) Modeling electron transfer thermodynamics in protein complexes: Interaction between two cytochromes c(3), *Biophys. J. 86*, 2773−2785.
43. Pieulle, L., Morelli, X., Gallice, P., Lojou, E., Barbier, P., Czjzek, M., Bianco, P., Guerlesquin, F., and Hatchikian, E. C. (2005) The type I/type II cytochrome c_3 complex: an electron transfer link in the hydrogen-sulfate reduction pathway, *J. Mol. Biol. 354*, 73−90.

BI0610294